

# Stability of Active Constraints Enforcement in Sensitive Regions Defined by Point-Clouds for Robotic Surgical Procedures

Theodora Kastritsi<sup>†,2</sup>, Dimitrios Papageorgiou<sup>1,2</sup>, Iason Sarantopoulos<sup>1,2</sup>, Zoe Doulgeri<sup>1,2</sup>  
and George A. Rovithakis<sup>1,2</sup>

**Abstract**—Robotic minimally invasive surgery provides images from the intraoperative field including organs and sensitive anatomic structures whose protection from non-voluntary destruction is imperative. To assist the surgeon, control methods that discourage motions towards these sensitive areas are advocated in the related literature. In this work, an active constraint controller is proposed and is proved to guarantee that sensitive/forbidden areas defined by a point cloud are never violated by the tool tip while the closed loop system remains passive and its state bounded under the exertion of a human guiding force. Experimental results are given utilizing a KUKA LWR4+ kinesthetically guided in a virtual surgical environment.

## I. INTRODUCTION

Robotic Minimally Invasive Surgery (RMIS) is a type of Minimally Invasive Surgery (MIS) which utilizes a master-slave manipulator system [1], [2]. MIS procedures are performed with elongated instruments through tiny incisions in the skin of the patient [3] thus minimum incurring intraoperative damage to the patients body. The advantages are many including the decreased cost of post-operative complications [4]. However, as surgeons in MIS manually operate the tools with their hands they may undergo fatigue in lengthy operations which deteriorate their performance. In an effort to overcome the problems of MIS while retaining its advantages, RMIS has been used [1]. RMIS is able to provide 3D vision, motion scaling, visual immersion and tremor filtration. Images from the intraoperative space are provided by an endoscopic camera as point-clouds in their raw-form. These images include organs and sensitive areas such as vessels and delicate tissues. To avoid involuntary destruction of these sensitive anatomic structures owing to the surgeon's strain, the implementation of control methods that discourage motions towards these sensitive areas has been proposed [5], [6]. Control methods that enforce Active Constraints (AC) or Virtual Fixtures (VF) are promising solutions among them.

Email addresses: tkastrit@ece.auth.gr, dimpapag@{iti/eng.auth}.gr, iasons@{iti/auth}.gr, doulgeri@{iti/eng.auth}.gr, robi@{iti/eng.auth}.gr

<sup>1</sup>Information Technologies Institute (ITI) Center of Research and Technology Hellas (CERTH) 57001 Thessaloniki, Greece.

<sup>2</sup>Department of Electrical and Computer Engineering, Aristotle University of Thessaloniki, Thessaloniki, 54124 Greece.

This work is funded by the EU Horizon 2020 research and innovation programme under grant agreement No 732515, project SMARTSurg.

<sup>†</sup>This research is co-financed by Greece and the European Union (European Social Fund- ESF) through the Operational Programme Human Resources Development, Education and Lifelong Learning in the context of the project Strengthening Human Resources Research Potential via Doctorate Research (MIS-5000432), implemented by the State Scholarships Foundation (IKY).

AC have been introduced in robotic autonomous operations to avoid obstacles while reaching a prespecified goal [7]. They have also been used as means to virtually restrict the robot operation in a confined workspace. Moreover, AC were utilized in physical human-robot interaction either as safety guarding or assistive tools; for example in [8] kinesthetic guidance along known paths was assisted by AC. In a telepresence system, AC were firstly used by Rosenberg [9]. However, in all the above works AC were defined via mathematical expressions of the constraint surface. In many cases, such an expression was possible since prototype geometric structures were assumed to contain areas or objects to be avoided. In surgical applications such an analytic expression may not be available or desired. Surgeons may need to operate close to forbidden areas thus circumscribed geometric structures are not effective means to this end. On the other hand, deriving analytic expressions of real organs and vessels is not an easy task particularly if a real time performance is sought. Thus in RMIS, AC have been defined using point clouds of the sensitive area but the enforcement of these constraints by the control action is not theoretically justified [10], [11].

This work intends to fill this gap by presenting a theoretically sound AC controller for surgical applications. It extends our previous work [8], which involved an analysis of the stability and non-constraint violation of previously proposed AC controllers for a physically guided robot given analytic expressions of the forbidden areas; simulation results with a 2-dof robot with a rotational and a prismatic joint were only given to validate the analysis. Such an analysis however, cannot be directly extended when the forbidden area is given as a point cloud. Our proposed controller utilizes the generally accepted practice of considering only the activated points which are continuously updated as the surgeon moves its tool, to include the region that is closest to the current tool position for reducing computational load. Nevertheless, the minimum distance utilized in [8] cannot be calculated owing to the lack of an analytic expression; hence the controller and the results of [8] are not directly applicable. The active constraint control law proposed in this work is proved to guarantee, for the first time to our knowledge, that constraints defined by point-clouds are never violated by the instrument tip and that the closed loop system is passive and its state is bounded and is validated by experiment.

The structure of the paper is as follows. Section II concerns the problem formulation while Section III details the proposed controller for active constraint enforcement.

Section IV presents the stability analysis of a kinesthetically guided robot under the proposed AC controller. Its performance is demonstrated and validated by experiments detailed in Section V in a use case involving a kidney and its adjacent vessels. Conclusions are drawn in Section VI. In the Appendix important theorems utilized in the stability analysis are reported.

## II. PROBLEM FORMULATION

Consider the dynamic model of a 3-dof non-redundant manipulator in the 3-dimensional operational space with gravity compensation and additive dissipative force under the kinesthetic guidance of a human force  $\mathbf{F}_h \in \mathbb{R}^3$  and the action of a control input  $\mathbf{u}_c \in \mathbb{R}^3$  that is designed to enforce active constraints:

$$\Lambda_p(\mathbf{p})\ddot{\mathbf{p}} + (\mathbf{C}_p(\mathbf{p}, \dot{\mathbf{p}}) + \mathbf{D}_d)\dot{\mathbf{p}} - \mathbf{u}_c = \mathbf{F}_h, \quad (1)$$

where

$$\Lambda_p(\mathbf{p}) = [\mathbf{J}(\mathbf{q})\Lambda^{-1}(\mathbf{q})\mathbf{J}^T(\mathbf{q})]^{-1}, \quad (2)$$

$$\mathbf{C}_p(\mathbf{p}, \dot{\mathbf{p}})\dot{\mathbf{p}} = \mathbf{J}^{-T}(\mathbf{q})\mathbf{C}(\mathbf{q}, \dot{\mathbf{q}})\dot{\mathbf{q}} - \Lambda_p(\mathbf{p})\dot{\mathbf{J}}(\mathbf{q})\dot{\mathbf{q}} \quad (3)$$

with  $\mathbf{p}(t), \dot{\mathbf{p}}(t) \in \mathbb{R}^3$  being the tool tip position and velocity of the robot,  $\mathbf{q}, \dot{\mathbf{q}} \in \mathbb{R}^3$  robot joint position and velocity,  $\mathbf{J}(\mathbf{q}) \in \mathbb{R}^{3 \times 3}$  the robot Jacobian,  $\Lambda(\mathbf{q}) \in \mathbb{R}^{3 \times 3}$  the manipulator's inertia matrix,  $\mathbf{C}(\mathbf{q}, \dot{\mathbf{q}}) \in \mathbb{R}^{3 \times 3}$  the Coriolis and centripetal matrix,  $\mathbf{D}_d \in \mathbb{R}^{3 \times 3}$  is a positive definite matrix of the desired damping. Notice that  $\Lambda_p$  is positive definite and the matrix  $\dot{\Lambda}_p - 2\mathbf{C}_p$  is skew symmetric.

It is assumed that the reconstructed surgical environment is provided as a 3-D point cloud from the endoscopic camera. It is also assumed that the operator (the surgeon) may select a subset of the points belonging to the sensitive region via an appropriately designed Graphical user interface (GUI) or by other means, as well as a subset of the points belonging to the region in which the surgeon intends to act. The former subset approximates the organ surfaces or delicate tissues that should not be violated by the robot's end-effector while the latter approximates the surface of the region within which the surgeon would like to move the robot tool tip freely. Let  $\mathcal{O}_s$  be the finite subset of points of the restricted region and  $\mathcal{A}_s$  the finite subset of points of the allowed region, which are disjoint sets. For simplicity and without loss of generality, consider all positions  $\mathbf{p}(t)$ ,  $\mathcal{O}_s$  and  $\mathcal{A}_s$  be expressed in the same coordinate system.

The *main objective* of this work is to control the robot so that it actively resists the human operator by exerting a repulsive force when he guides the end-effector near the restricted region not allowing to ever enter it.

The approximation of the constrained region's surface by a finite set of points  $\mathcal{O}_s$ , results in an empty space between them. To achieve our main objective we initially create spheres, centered at each point of the constrained region's surface with radius  $d_c$  such that all empty space is covered by the overlapping spheres. In particular, if  $\rho \in \mathbb{R}^+$  is the density of  $\mathcal{O}_s$  in points per  $cm^3$  by selecting  $d_c = \frac{\sqrt{3}}{2\sqrt[3]{\rho}}$  we can guarantee that these empty spaces are covered (Fig. 1). Notice that the radius  $d_c$  depends on the density of  $\mathcal{O}_s$ ,

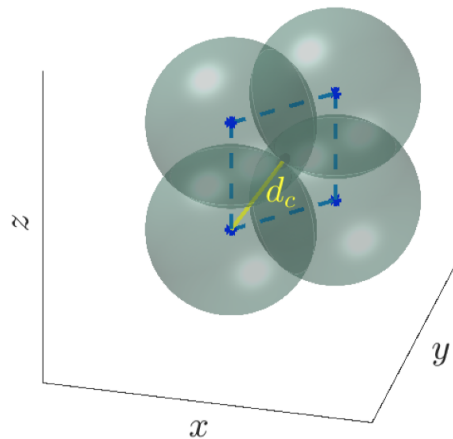


Fig. 1. Visualization of the spheres created around each point of the constrained region's surface.

which is considered known and homogeneous. In this way the constrained surface can be defined as the boundary of the overlapping spheres  $\partial\mathcal{O}_c$  where the set  $\mathcal{O}_c$  is defined as follows:

$$\mathcal{O}_c = \bigcup_{\mathbf{p}_i \in \mathcal{O}_s} \{\mathbf{p} \in \mathbb{R}^3 : \|\mathbf{p} - \mathbf{p}_i\| \leq d_c\}. \quad (4)$$

Consequently, the constraint-free space  $\Omega$  is

$$\Omega = \mathbb{R}^3 - \mathcal{O}_c. \quad (5)$$

Besides the main control objective defined previously, the robot should maintain a passivity property and state boundedness irrespective of whether its tip is away or near the constrained space.

## III. THE PROPOSED AC CONTROLLER

Let us now consider the nearest to the end-effector spheres defined as the spheres with its surfaces within a predefined distance  $d_0 \in \mathbb{R}^+$  from the end-effector. In particular, consider the set of the neighboring to the tool tip, sphere centers  $\mathcal{C}$ , which is defined as follows:

$$\mathcal{C} = \{\mathbf{p}_i \in \mathcal{O}_s : \|\mathbf{p} - \mathbf{p}_i\| \leq (d_0 + d_c)\} \quad (6)$$

Only these spheres will only be activated with respect to the active constraints instead of the whole set thus reducing the computational load of the method. In practice, to calculate the set  $\mathcal{C}$ , we use the commonly available  $k$ -d tree search [12], [13], i.e. we create a  $k$ -d tree from the points of  $\mathcal{O}_s$ , and we search for all the points close to tool point.

For each sphere with a centre in  $\mathcal{C}$ , we propose the following artificial potential shown in Fig. 2:

$$V_i = \frac{1}{2} \ln \left( \frac{1}{1 - \psi_i} \right)^2 \quad (7)$$

where

$$\psi_i = \frac{(\|\mathbf{p} - \mathbf{p}_i\| - (d_0 + d_c))^2}{d_0^2} \quad (8)$$

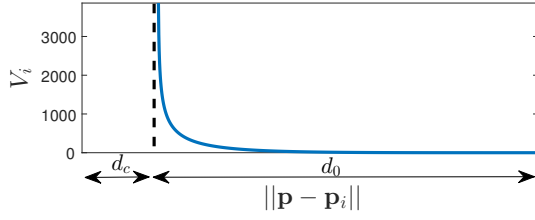


Fig. 2. The AP function used in this work.

Notice that the minimum Euclidean distance between the robot's position and the restricted region utilized in [8] cannot be used in this case since an analytic expression for the forbidden region is not available. Further notice that  $V_i < \infty$  if and only if  $\psi_i < 1$ . Hence, owing to (6)  $\psi_i < 1$  if and only if  $\|\mathbf{p} - \mathbf{p}_i\| > d_c$  (Fig. 2).

*Remark 1:* Notice that parameter  $d_0$  is related to the total area of the influence of the potential field. Hence the value  $d_0$  should be set such that no repulsive forces are exerted within the allowed region  $\mathcal{A}_s$ . In particular,  $d_0$  is selected as  $d_0 = d_m - d_c$  with  $d_m$  being the minimum distance between the sets  $\mathcal{O}_s$  and  $\mathcal{A}_s$ :  $d_m = \min\{\|\mathbf{p}_i - \mathbf{p}_a\| : \mathbf{p}_i \in \mathcal{O}_s, \mathbf{p}_a \in \mathcal{A}_s\}$ .

The constrained surface defined by the spheres in  $\mathcal{C}$  is enforced by the sum of repulsive forces  $\mathbf{f}_i \in \mathbb{R}^3$  produced by the gradient of the Artificial Potential field  $V_i$ :

$$\mathbf{f}_i = -\frac{\partial V_i}{\partial \mathbf{p}}. \quad (9)$$

which for the proposed potential field is given by:

$$\mathbf{f}_i = \frac{2}{d_0^2(1-\psi_i)} \ln\left(\frac{1}{1-\psi_i}\right) \mathbf{e}_i, \quad \forall \mathbf{p}_i \in \mathcal{C} \quad (10)$$

where  $\mathbf{e}_i \in \mathbb{R}^3$  is given by:

$$\mathbf{e}_i = ((d_0 + d_c) - \|\mathbf{p} - \mathbf{p}_i\|) \frac{\mathbf{p} - \mathbf{p}_i}{\|\mathbf{p} - \mathbf{p}_i\|} \quad (11)$$

expressing the minimum distance between the robot tool point and the sphere surface along the direction of the line connecting the sphere's center to the tool point.

The proposed AP function (7) has the following properties:

- $V_i(\mathbf{p}) = V(\|\mathbf{p} - \mathbf{p}_i\|)$  is a positive continuously differentiable scalar function, for all  $\|\mathbf{p} - \mathbf{p}_i\| \in (d_c, d_0 + d_c]$ ;
- $V_i(\mathbf{p}) \rightarrow \infty$  if only if  $\|\mathbf{p} - \mathbf{p}_i\| \rightarrow d_c$ ;
- $\frac{\partial V_i(\mathbf{p})}{\partial \mathbf{p}}$  is zero if and only if  $\|\mathbf{p} - \mathbf{p}_i\| = d_c + d_0$ .

Any AP that satisfies the above properties can be used instead of the proposed AP.

Finally, the total repulsive force on the end-effector, which is utilized as a control signal, is the sum of the forces  $\mathbf{f}_i$  produced by each artificial potential field of the neighboring spheres, i.e.:

$$\mathbf{u}_c = k \sum_{\mathbf{p}_i \in \mathcal{C}} \mathbf{f}_i \quad (12)$$

where  $k > 0$  is a scalar gain.

*Remark 2:* Notice that the definition of  $\mathcal{C}$  in (6) implies that the term  $(\|\mathbf{p} - \mathbf{p}_i\| - (d_0 + d_c))$  will never be negative,

since only surface points that belong to  $\mathcal{C}$  are taken into account. Furthermore, any new  $\mathbf{p}_i$  entering  $\mathcal{C}$  will contribute continuously in  $\mathbf{u}_c$ , as the corresponding repulsive force  $\mathbf{f}_i$  is initially zero.

The above methodology can be described in pseudocode form as shown below:

```

while controller runs do
   $\mathbf{p} \leftarrow$  End-effector position
   $\mathcal{O}_s \leftarrow$  Constraint's point cloud
  Create kd-tree from  $\mathcal{O}_s$ 
   $\mathcal{C} \leftarrow$  Search points in  $k$ -d tree with distance from  $\mathbf{p}$ 
  below  $d_0 + d_c$ 
   $\mathbf{u}_c \leftarrow 0$ 
  for  $\mathbf{p}_i \in \mathcal{C}$  do
    Calculate  $\mathbf{f}_i$  from Eq. (9)
     $\mathbf{u}_c \leftarrow \mathbf{u}_c + k\mathbf{f}_i$ 
  end for
end while

```

*Remark 3:* Notice that the approximation of the constraint surface with spheres can produce ripples in the repulsive force signal if a motion parallel to the surface and within the area of influence of the AC is performed. Such a motion however is not expected since the surgeon has already specified his working space (the allowed region) within which repulsive forces are not exerted by design. Therefore the proposed method does not hinder the proper execution of the task.

#### IV. STABILITY ANALYSIS

As long as the active constraint controller is enabled i.e.,

$$\mathbf{p} \in \Omega_c = \bigcup_{\mathbf{p}_i \in \mathcal{O}_s} \{\mathbf{p} \in \Omega : \|\mathbf{p} - \mathbf{p}_i\| \leq d_c + d_0\} \quad (13)$$

we investigate the system's passivity with respect to its output  $\dot{\mathbf{p}}$  and state boundedness under the presence of an external input force  $\mathbf{F}_h$ , which is assumed to be of finite energy. The latter is a reasonable assumption as this force is exerted by a human. To proceed with the stability analysis, we initially write system (1) in state-space. To this purpose we define  $\xi = \sum_{\mathbf{p}_i \in \mathcal{C}} V_i(\mathbf{p})$  as an internal system state. Then, utilizing the state vector:

$$\mathbf{s} = [\dot{\mathbf{p}} \ \mathbf{p} \ \xi]^T \in \mathbb{R}^7 \quad (14)$$

we can define the initial value problem:

$$\dot{\mathbf{s}} = \mathbf{g}(\mathbf{s}, \mathbf{F}_h(t)), \mathbf{s}_0 = \mathbf{s}(t_0) \in D \quad (15)$$

where  $D \triangleq \mathbb{R}^3 \times \Omega_c \times \mathbb{R}$

$$\mathbf{g}(\mathbf{s}, \mathbf{F}_h) = \begin{bmatrix} \Lambda_p^{-1}(-(\mathbf{C}_p + \mathbf{D}_d)\dot{\mathbf{p}} + \mathbf{F}_h(t) + \mathbf{u}_c) \\ \dot{\mathbf{p}} \\ (\sum_{\mathbf{p}_i \in \mathcal{C}} \frac{\partial V_i}{\partial \mathbf{p}})^T \dot{\mathbf{p}} \end{bmatrix}.$$

*Theorem 1:* (i) As long as  $\mathbf{p} \in \Omega_c$  the following statements are valid:

- Under the exertion of the external input  $\mathbf{F}_h$ , (15) is strictly output passive with respect to  $\dot{\mathbf{p}}$ .
- There exists a compact subset  $D_1$  of  $D$  such that  $\mathbf{s} \in D_1$ .

(ii) Whenever  $\mathbf{p} \in \Omega \wedge \mathbf{p} \notin \Omega_c$  the robotic system (1) is 0-GAS and strictly output passive with respect to  $\dot{\mathbf{p}}$ .

*Proof:* (i) Let  $\mathbf{p}(t) \in \Omega_c$ , for all  $t \in [t_0, T)$ . By definition  $\mathbf{g}(\mathbf{s}, \mathbf{F}_h(t))$  is continuous in  $t$  and locally Lipschitz with respect to  $\mathbf{s}$ . Owing to Theorem 3.1, [14], there exists a time instance some  $\tau < T$  such that (15) has a unique solution in a maximal time interval  $[t_0, \tau)$  with  $\tau \in (t_0, T]$  i.e.,  $\mathbf{s}(t) \in D$ , for all  $t \in [t_0, \tau)$ .

We assume the following candidate Lyapunov-like function:

$$V = \frac{1}{2} \dot{\mathbf{p}}^T \Lambda_p \dot{\mathbf{p}} + k \sum_{\mathbf{p}_i \in \mathcal{C}} V_i(\mathbf{p}) \geq 0. \quad (16)$$

Taking the time derivative for all  $t \in [t_0, \tau)$  of (16) yields

$$\dot{V} = \frac{1}{2} \dot{\mathbf{p}}^T \dot{\Lambda}_p \dot{\mathbf{p}} + \dot{\mathbf{p}}^T \Lambda_p \dot{\mathbf{p}} + k \sum_{\mathbf{p}_i \in \mathcal{C}} \frac{\partial V_i(\mathbf{p})}{\partial \mathbf{p}} \dot{\mathbf{p}}. \quad (17)$$

Substituting  $\Lambda_p \ddot{\mathbf{p}}$  from (1) in (17), and utilizing the skew-symmetry of matrix  $(\dot{\Lambda}_p - 2\mathbf{C}_p)$ , yields:

$$\begin{aligned} \dot{V} &= -\dot{\mathbf{p}}^T \mathbf{D}_d \dot{\mathbf{p}} + \mathbf{F}_h^T \dot{\mathbf{p}} \\ &\leq -\lambda_{\min}(\mathbf{D}_d) \dot{\mathbf{p}}^T \dot{\mathbf{p}} + \mathbf{F}_h^T \dot{\mathbf{p}}, \quad \forall t \in [t_0, \tau) \end{aligned} \quad (18)$$

where  $\lambda_{\min}(\cdot)$  is the minimum eigenvalue of a matrix. Hence, system (15) is strictly output passive for all  $t \in [t_0, \tau)$ , with respect to  $\dot{\mathbf{p}}$  (see *Definition 2* including in the Appendix).

Rewriting (18) by completing the squares, yields:

$$\begin{aligned} \dot{V} &= -\|\sqrt{\mathbf{D}_d} \dot{\mathbf{p}} - \frac{1}{2} \sqrt{\mathbf{D}_d}^{-1} \mathbf{F}_h\|^2 + \frac{1}{4} \mathbf{F}_h^T \mathbf{D}_d^{-1} \mathbf{F}_h \\ &\leq \frac{1}{4} \mathbf{F}_h^T \mathbf{D}_d^{-1} \mathbf{F}_h, \quad \forall t \in [t_0, \tau). \end{aligned} \quad (19)$$

Notice that  $\mathbf{F}_h$  represents the force applied by the human to guide the robot. Thus,  $\mathbf{F}_h$  is bounded and therefore  $\mathbf{F}_h^T \mathbf{D}_d^{-1} \mathbf{F}_h$  is also a bounded function of time. Additionally the human forces have bounded energy so by integrating equation (19) we get:

$$V \leq V(t_0) + \int_{t_0}^t \frac{1}{4} \mathbf{F}_h^T \mathbf{D}_d^{-1} \mathbf{F}_h < \infty, \quad \forall t \in [t_0, \tau) \quad (20)$$

Thus, states  $\xi$  and  $\dot{\mathbf{p}}$  are bounded under the exertion of human force for all  $t \in [t_0, \tau)$ . Stated otherwise there exist compact sets  $\Omega_\xi, \Omega_v$  such that  $\xi \in \Omega_\xi \subset \mathbb{R}$  and  $\dot{\mathbf{p}} \in \Omega_v \subset \mathbb{R}^3$  for all  $t \in [t_0, \tau)$ . As a consequence, there exists a positive constance  $\bar{\varepsilon}_i$  such that  $V_i \leq \bar{\varepsilon}_i$ , for all  $t \in [t_0, \tau)$ , which for the logarithmic function defined in (7) and owing to (6) it yields:

$$0 \leq 1 - \frac{1}{e^{\sqrt{2\bar{\varepsilon}_i}}} < 1, \quad \forall t \in [t_0, \tau) \text{ and } i = 1, \dots, M,$$

Hence (8) yields that  $\|\mathbf{p} - \mathbf{p}_i\| \geq d_r > d_c$ ,  $i \in \{1, \dots, M\}$  for all  $t \in [t_0, \tau)$ . However,  $\mathbf{p} \in \Omega_c$  for all  $t \in [t_0, \tau)$ . Therefore  $\|\mathbf{p} - \mathbf{p}_i\| \leq d_c + d_0$  for all  $t \in [t_0, \tau)$ . Thus,  $\mathbf{p}$  evolves in a compact subset  $\Omega_1$  of  $\Omega_c$  and consequently  $\mathbf{s}(t) \in D_1 \triangleq \Omega_v \times \Omega_1 \times \Omega_\xi$ , a compact subset of  $D$  for all  $t \in [t_0, \tau)$ . Using Theorem 3.3 of [14] we can conclude that  $\tau$  can be extended to  $T$ , thus proving the i-part of the theorem.

We have proved that as long as  $\mathbf{p} \in \Omega_c$  the constraints are not violated and the robot's states are bounded. In addition the robot possess a passivity property.

(ii) Whenever  $\mathbf{p} \in \Omega \wedge \mathbf{p} \notin \Omega_c$ , then  $\mathbf{u}_c = \mathbf{0}$  and (1) becomes

$$\Lambda_p(\mathbf{p}) \ddot{\mathbf{p}} + (\mathbf{C}_p(\mathbf{p}, \dot{\mathbf{p}}) + \mathbf{D}_d) \dot{\mathbf{p}} = \mathbf{F}_h. \quad (21)$$

It is not difficult to verify using the Lyapunov-like function  $W = \frac{1}{2} \dot{\mathbf{p}}^T \Lambda_p \dot{\mathbf{p}}$  that  $\dot{\mathbf{p}}$  converges exponentially to zero when  $\mathbf{F}_h = \mathbf{0}$ . Consequently, employing Lemma 1 of Appendix, we conclude that  $\mathbf{p}$  also converges to a constant, proving that (21) is 0-GAS (see *Definition 3* of the Appendix). Moreover, for  $\mathbf{F}_h \neq \mathbf{0}$  and following the line of analysis used to prove the i- part of the theorem, (21) is again strictly output passive w.r.t  $\dot{\mathbf{p}}$ . Thus we have proved the ii-part of the Theorem. ■

In the aforementioned analysis it should be stressed that the input  $\mathbf{u}_c + \mathbf{F}_h$  (when  $\mathbf{p} \in \Omega_c$ ) and  $\mathbf{F}_h$  (when  $\mathbf{p} \in \Omega \wedge \mathbf{p} \notin \Omega_c$ ) preserves its continuously as we enter or leave  $\Omega_c$ . Thus, avoiding possible instability effects that may be caused otherwise.

## V. EXPERIMENT

To demonstrate the effectiveness of the proposed methodology, we consider a surgical procedure where a user want to move the tool tip in the vicinity of a kidney but not its adjacent vessels via kinesthetic guidance of a master device.

### A. Experimental Setup

To emulate a master slave setup, a 7-dof KUKA LWR4+ robotic manipulator was used as the master and an identical virtual manipulator as the slave device. A 3-D point cloud of an internal human organ is imported into a virtual scene and displayed to the user together with the slave manipulator. The user has the opportunity to change the current view via zooming in/out, translating or rotating the view. The user guides the master by its tool by looking at the virtual scene. The master's joint positions are sent to the virtual KUKA. When a repulsive force is generated at the virtual scene it is applied to the master tool tip to provide the user with the required haptic feedback. The repulsive force is visualized in the scene. A wrist force sensor at the master device is used to measure the human force for the only purpose of visualizing it in the virtual scene. The proposed methodology is implemented in C++ using the FRI library with control frequency  $f_s = 250$  Hz.

We consider the case which the user performs the removal of a kidney tumor and the surgical tool must not touch the adjacent vessels. In this experiment, the user was asked to guide the tool tip, via kinesthetic guidance of the master device, initially on the kidney and then in the area of the vessels. The area of the vessels define the constrained region and their point cloud defines the set  $\mathcal{O}_s$  (Fig. 3a). Initially the point cloud of the vessels is down sampled to increase computational performance. The radius of the spheres  $d_c = 1.768$  mm is selected to cover the empty space based on the cloud's density. This implies that the tool tip

cannot be guided in a distance equal or smaller of 1.768 mm from the vessels. In this experiment, the distance  $d_0$  for the activation of the repulsive force, is set to the value  $d_0 = 2.3$  cm. This implies that the user will start to feel forces from the controller when the tip has a distance from the sphere centers less  $d_0 + d_c = 2.4768$  cm. Finally, we used  $k = 0.03$  as the gain of the controller.

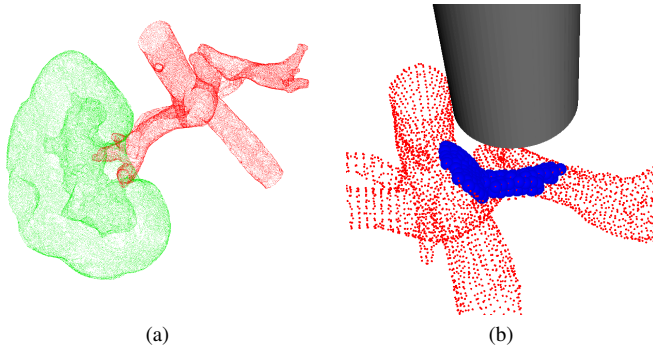


Fig. 3. The point cloud of the scene and the nearest spheres to the tool point. (a) The point cloud of the constrained region of the vessels (red color) and the operable region of the kidney (green color). (b) The nearest to the tool point spheres (blue color).

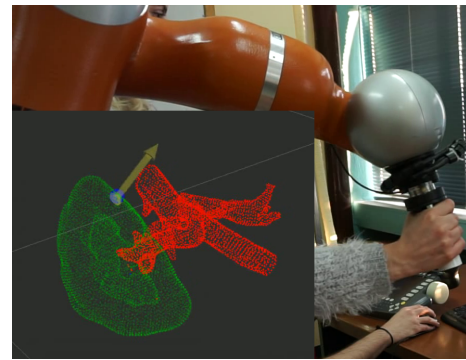
### B. Experimental Results

When the user guides the tool tip in the area of the kidney the distance of the end-effector from  $\mathcal{O}_s$  is large enough and thus Eq. (6) results in  $\mathcal{C}$  being an empty set and no repulsive forces are generated (Fig. 4a). When the user attempts to reach the vessels, spheres within the selected threshold  $d_0$  are found (the blue region in Fig. 3b) and their Artificial Potential fields starts to produce forces (purple arrow in Fig. 4b). When the operator tries to penetrate the constrained region by exerting high forces (yellow arrow in Fig. 4c), he fails, as the controller produces a high repulsive force close to the vessels (purple arrow in Fig. 4c).

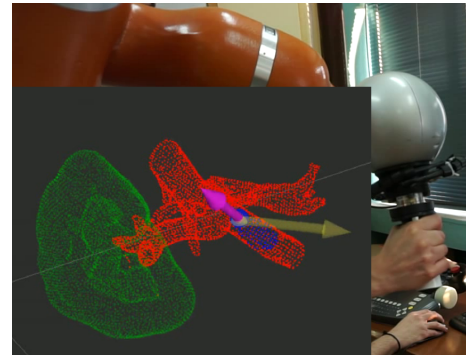
Fig. 5 depicts the norm of the repulsive force along with the measured minimum distance of the end-effector from the points in  $\mathcal{C}$  during the time the operator is guiding the tip close to the forbidden area and hence the active constraints have been activated. The repulsive force is the result of all repulsive forces produced by the spheres belonging in  $\mathcal{C}$  (Eq. (9)). Its norm is mainly determined from the closest to the tip sphere. Notice that the end-effector never touches the constrained surface (the minimum distance never goes close to zero). Further notice how the maximum of the repulsive force occurs at time  $t = 37sec$  where the tool reached a position close to the constraints (approximately at 1.1cm) which is the case shown in Fig. 4c. The online video of the experiment is available at <https://youtu.be/4qJ4I1uHtSc>.

## VI. CONCLUSION

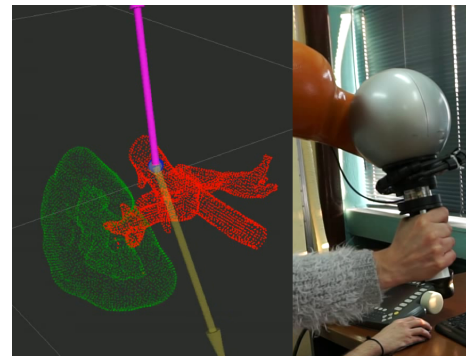
A controller was proposed, to guarantee that the tool tip of a surgical robot will not touch a constraint surface defined by a point cloud. Artificial Potential fields are utilized to produce repulsive forces away from the constraints that are



(a)



(b)



(c)

Fig. 4. Experiment with the free-to-move region of a kidney (green) and the constrained region of human vessels (red). With yellow arrow the force exerted by the operator on the robot, with purple arrow the repulsive force  $\mathbf{f}$  of the controller, sensed by the human and with blue points the set  $\mathcal{O}_s$ . (a) The operator moves along the area of the kidney, where no repulsive force is generated. (b) The operator moves the robot close to vessels starting to feel the resistance of the repulsive force. (c) The operator tries to violate the active constraint by applying high forces, which are resisted by high repulsive forces.

activated around the points closer to the tool. The closed-loop system is proven strictly output passive with respect to the end-effector velocity guaranteeing constraint satisfaction. Experiments are conducted using a KUKA LWR4+ robot, demonstrating the effectiveness of the proposed method. Extension of this work on calculating the repulsive force by taking into consideration the whole tool body, instead of only the tool point, can be found in [15].

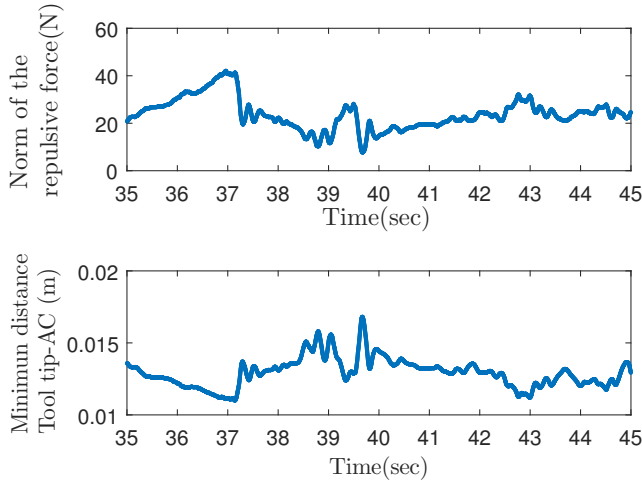


Fig. 5. Diagram of the norm of the repulsive force and the minimum distance of the end-effector from the points on the constrained region surface.

## APPENDIX

### A. Preliminaries about passivity and stability

Consider a nonlinear system

$$\begin{aligned}\dot{\boldsymbol{\varphi}} &= \mathbf{W}(\boldsymbol{\varphi}, \mathbf{u}), \boldsymbol{\varphi}_0 = \boldsymbol{\varphi}(t_0) \\ \mathbf{y} &= \mathbf{H}(\boldsymbol{\varphi})\end{aligned}\quad (22)$$

where  $\boldsymbol{\varphi} \in \mathbb{R}^n$  is the state,  $\mathbf{y} \in \mathbb{R}^p$  is the output and  $\mathbf{u} \in \mathbb{R}^m$  is the input of system (22).

*Definition 1:* Dissipative system [16]

System (22) is said to be dissipative with supply rate  $w(\boldsymbol{\varphi}, \mathbf{y}, \mathbf{u}) : \mathbb{R}^n \times \mathbb{R}^p \times \mathbb{R}^m \rightarrow \mathbb{R}$ , if there exists a positive semidefinite smooth real function  $S(\boldsymbol{\varphi}) : \mathbb{R}^n \rightarrow \mathbb{R}$  such that:

$$\dot{S}(\boldsymbol{\varphi}) \leq w(\boldsymbol{\varphi}, \mathbf{y}, \mathbf{u}). \quad (23)$$

*Definition 2:* Strictly output passive system [17]

System (22) with  $p = m$  is said to be strictly output passive, if it is dissipative with respect to supply rate  $w(\mathbf{u}, \mathbf{y}) = \mathbf{u}^T \mathbf{y} - \rho \mathbf{y}^T \mathbf{y}$ , for  $\rho > 0$ .

*Definition 3:* 0-GAS system [18]

System (22) is said to be 0-GAS if the 0-input system  $\dot{\boldsymbol{\varphi}} = \mathbf{W}(\boldsymbol{\varphi}, 0)$  is globally asymptotically stable.

### B. Convergence

*Lemma 1:* Suppose  $\mathbf{c} : [0, \infty) \rightarrow \mathbb{R}^w$  and satisfies  $\|\mathbf{c}(t)\| \leq ne^{-\lambda t}$  for all  $t \in [0, \infty)$  where  $n, \lambda > 0$ . Then  $\int_0^\infty \mathbf{c}(t)dt$  converges.

*Proof:* Since we have  $0 \leq \|\mathbf{c}(t)\| \leq ne^{-\lambda t}$  for all  $t \in [0, \infty)$  and  $\int_0^\infty ne^{-\lambda t}dt$  converges to a constant, by the direct comparison test (*Theorem 2*) we obtain that  $\int_0^\infty \|\mathbf{c}(t)\|dt$  converges to a constant. Then  $0 \leq \|c_i(t)\| \leq \|\mathbf{c}(t)\|^1$ ; thus using again the direct comparison test we obtain that  $\int_0^\infty \|c_i(t)\|dt$  is convergent to a constant. However, using the *Theorem 3*,  $\int_0^\infty c_i(t)dt$  converges to a constant and therefore  $\int_0^\infty \mathbf{c}(t)dt$  converges to a constant as well. ■

<sup>1</sup> $c_i(t)$  denoting the  $i$ th element of the  $\mathbf{c}(t)$  vector.

*Theorem 2:* Direct Comparison Test [19]

If  $0 \leq z(x) \leq b(x)$  for all  $x \in [0, \infty)$  and  $\int_0^\infty b(x)dx$  converges to a constant then  $\int_0^\infty z(x)dx$  converges to a constant.

*Theorem 3:* Convergence of Improper Integral [20]

If an improper integral  $\int_a^\infty |f(x)|dx$  converges to a constant then  $\int_a^\infty f(x)dx$  converges to a constant.

## REFERENCES

- [1] J. W. Hill, P. S. Green, J. F. Jensen, Y. Gorf, and A. S. Shah, "Telepresence surgery demonstration system," in *Proceedings of the 1994 IEEE International Conference on Robotics and Automation*, May 1994, pp. 2302–2307 vol.3.
- [2] P. S. Green, J. W. Hill, J. F. Jensen, and A. Shah, "Telepresence surgery," *IEEE Engineering in Medicine and Biology Magazine*, vol. 14, no. 3, pp. 324–329, May 1995.
- [3] Q. Xie, J. Zhang, F. Lu, H. Wu, Z. Chen, and F. Jian, "Minimally invasive versus open transforaminal lumbar interbody fusion in obese patients: a meta-analysis," *BMC musculoskeletal disorders*, vol. 19, no. 1, p. 15, 2018.
- [4] S. Parker, O. Adogwa, T. F. Witham, O. Aaronson, J. Cheng, and M. McGirt, "Post-operative infection after minimally invasive versus open transforaminal lumbar interbody fusion (tlif): literature review and cost analysis," *min-Minimally Invasive Neurosurgery*, vol. 54, no. 01, pp. 33–37, 2011.
- [5] S. A. Bowyer, B. L. Davies, and F. R. y Baena, "Active constraints/virtual fixtures: A survey," *IEEE Transactions on Robotics*, vol. 30, no. 1, pp. 138–157, Feb 2014.
- [6] S. A. Bowyer and F. R. y Baena, "Dissipative control for physical human-robot interaction," *IEEE Transactions on Robotics*, vol. 31, no. 6, pp. 1281–1293, 2015.
- [7] O. Khatib and J. Le Maitre, "Dynamic control of manipulators operating in a complex environment," in *3rd CISM-IFTOMM Symp On Theory and Practice of Robots and Manipulators*, vol. 267, 1978.
- [8] T. Kastritsi, D. Papageorgiou, and Z. Doulgeri, "On the stability of robot kinesthetic guidance in the presence of active constraints," in *2018 European Control Conference (ECC)*, June 2018, pp. 622–627.
- [9] L. B. Rosenberg, "The use of virtual fixtures as perceptual overlays to enhance operator performance in remote environments." DTIC Document, Tech. Rep., 1992.
- [10] F. Rydn and H. J. Chizeck, "Forbidden-region virtual fixtures from streaming point clouds: Remotely touching and protecting a beating heart," in *2012 IEEE/RSJ International Conference on Intelligent Robots and Systems*, Oct 2012, pp. 3308–3313.
- [11] K. Leibrandt, H. J. Marcus, K. Kwok, and G. Yang, "Implicit active constraints for a compliant surgical manipulator," in *2014 IEEE International Conference on Robotics and Automation (ICRA)*, May 2014, pp. 276–283.
- [12] J. L. Bentley, "Multidimensional binary search trees used for associative searching," *Communications of the ACM*, vol. 18, no. 9, pp. 509–517, 1975.
- [13] R. B. Rusu and S. Cousins, "3D is here: Point Cloud Library (PCL)," in *IEEE International Conference on Robotics and Automation (ICRA)*, Shanghai, China, May 9-13 2011.
- [14] H. Khalil, *Nonlinear Systems*, 3rd ed. Prentice Hall, 2002.
- [15] T. Kastritsi, D. Papageorgiou, I. Sarantopoulos, S. Stavridis, Z. Doulgeri, and G. Rovithakis, "Guaranteed active constraints enforcement on pointcloud-approximated regions for surgical applications," in *IEEE International Conference on Robotics and Automation (ICRA)(accepted)*, Montreal, Canada, May 20-24 2019.
- [16] C. Ebenbauer, T. Raff, and F. Allgöwer, "Dissipation inequalities in systems theory: An introduction and recent results," in *Invited Lectures of the International Congress on Industrial and Applied Mathematics*, vol. 2007, 2009, pp. 23–42.
- [17] J. Bao, P. L. Lee, and B. E. Ydstie, "Process control: the passive systems approach." Ph.D. dissertation, Springer-Verlag, 2010.
- [18] D. Angeli, E. D. Sontag, and Y. Wang, "A characterization of integral input-to-state stability," *IEEE Transactions on Automatic Control*, vol. 45, no. 6, pp. 1082–1097, 2000.
- [19] G. B. Thomas, M. D. Weir, J. Hass, C. Heil, and A. Behn, "Thomas' calculus early transcendentals, 13th edition." Pearson, p. 510.
- [20] R. C. Wrede and M. R. Spiegel, "Advanced calculus, second edition." McGraw-Hill New York, pp. 309,319.